

Dynamics properties of polymer solutions (I). Dilute–semidilute transition

I.M. Irurzun^a, R.V. Figini^a, M. Marx-Figini^a, J.R. Grigera^{b,*}

^a*Instituto de Investigaciones Fisicoquímicas Teóricas y Aplicadas (INIFTA) Universidad Nacional de La Plata- CONICET, cc 16 suc4 1900 La Plata, Argentina*

^b*Instituto de Física de Líquidos y Sistemas Biológicos, IFLYSIB (UNLP-CONICET-CIC) and Departamento de Ciencias Biológicas, Universidad Nacional de La Plata, c.c. 565, 1900 La Plata, Argentina*

Received 5 October 1998; received in revised form 3 March 1999; accepted 8 March 1999

Abstract

Measurements of viscosity and dielectric relaxation were carried out using several solutions of cellulose trinitrate polymer in isophorone in the dilute and the semidilute regime. In each case, the renormalization group theory was applied to the data using the De Gennes's blobs model for connecting dynamic and conformational quantities. There was adequate agreement between the experimental results and the theoretical predictions to show universal behavior. The values of β were independent of both molecular weight and polymer concentration and could be used to describe a variety of dynamic properties. These findings suggest that only one scaling variable is necessary for such purposes. © 1999 Elsevier Science Ltd. All rights reserved.

Keywords: Polymers; Dielectric relaxation; Viscosity

1. Introduction

Linear polymers in good solvents exhibit universal behavior over the entire range from the dilute to the semidilute regime [1,2]. At both extremes, limiting power laws that can be derived from scaling arguments apply [3]. However, in the transition zone, the universal relationships take on a more complicated form, and powerful renormalization techniques become necessary to derive limiting power laws from a microscopic model of the system.

The conformational and thermodynamic properties of linear polymers in solution are reasonably well understood [4]. It is accepted that the progression towards a semidilute regime implies the screening of excluded volume interactions which arise when the polymer chains entangle. In contrast, as a consequence of the screening of hydrodynamic interactions, a description of the dynamic properties is more difficult. Although Shiwa et al. [5–7] developed a renormalization group procedure designed specifically to address viscosity and relaxation times, the problem is not yet fully understood, especially in the transition zone.

In this paper we present experimental data obtained from polymers in solution showing Newtonian viscosity and dielectric relaxation times throughout the dilute-to-semidilute

crossover. We analyzed our results using the renormalization group scheme developed by Schäfer [8,9], which enabled us to compute both the osmotic pressure and the gyration radius. In order to compare the experimental results with theoretical predictions, it was necessary to establish relationships between the conformational and dynamic properties. We made this connection using the scale arguments from De Gennes's blobs model.

Elsewhere, we used the same scheme to describe both the thermodynamic and rheological properties in binary and ternary solutions (for the development of Schäfer's theory to ternary solutions, see Refs. [10–14]), thereby obtaining a unified picture for the description of all of these systems.

2. Theoretical background

It has been well established experimentally that in the range from a dilute to a semidilute regime, the macroscopic properties of polymer solutions are universal functions of an overlap parameter, c/c^* , where c is the concentration of polymer and c^* is a critical concentration at which the polymer coils begin to overlap [15,16] and is defined as

$$c^* = \frac{3M}{4\pi S_{G,0}^3 N_A}, \quad (1)$$

where M is the molar mass of the solute, N_A is Avogadro's number, and $S_{G,0}$ is the gyration radius of an ideal chain.

*Corresponding author. Tel.: +54-221-425-49-04; +54-221-423-32-83; fax: +54-21-25-73-17.

E-mail address: grigera@iflysisib1.unlp.edu.ar (J.R. Grigera)

Schäfer [8,9] has developed a protocol that applies the renormalization group theory to the description of the universal conformational and thermodynamic properties of polymer solutions. This theory provides for unified treatment of the temperature and concentration crossover of the excluded volume interactions and thus presents a single computational scheme for all accessible physical quantities covering a full universal regime. The system was described using the well-known Gaussian model with excluded volume interactions. The polymer chain was characterized by a microscopic length l and by a quantity μ ,¹ which represents the strength of the two-body interaction in the cluster expansion. The solution was characterized by the number-concentration of polymer chains (c_p), a number-averaged chain length (N) and a chain length distribution ($P(n)$).

The renormalization group procedure allows one to obtain the changes in μ and N that occur with changes in scale as $l \rightarrow l/\lambda$. In the scheme developed by Schäfer, who used a normalized parameter f instead of μ , the value of f goes from 0, in the Θ -state, to 1 at the excluded volume limit.

The screening of excluded volume interactions takes into account the fact that the dilatation of l must be carried out until it essentially coincides with the correlation length ξ (note that ξ approaches to R_g in the infinite dilute limit). As ξ depends on both the molecular weight and the concentration, this condition tends to fix λ (and introduces a new variable (w) describing the concentration crossover. Here, w goes from 0 at the dilute limit to 1 at the semidilute limit.

Thus, the unrenormalized variables $c_l (= c_p N)$ and N can be mapped to the renormalized scaling field variables, w and f . In the mapping procedure, the microscopic characteristics are absorbed into two non-universal scale functions, s_N and s_l . Once the values of these functions are fixed, the c_l and N dependence becomes universal, and all scaling functions can be expressed in terms of w and f . A crossover diagram [9] can then be constructed plotting a given quantity as function of w and f . In such a diagram, the experimental data are plotted so that variation of the property of interest with c_l and N is indicated. In particular, if one starts from a dilute solution ($w = 1$) in the excluded volume regime ($f = 1$) and increases the concentration (c_l), a double crossover can be observed: there is an initial concentration transition ($w = 1$ to $w = 0$) in the excluded volume regime ($f = 1$) that is followed by a temperature crossover in the semidilute regime. This path is followed by the experimental results which start at $w = 1$ and $f = 1$ and almost reach the semidilute, excluded volume limit ($w = 0, f = 1$), and then go sharply to $f = 0$ in the semidilute regime ($w = 0$). As a consequence, the equations valid at $f = 1$ could be used over the entire concentration range covered by the present experiments (see details in Ref. [9]).

¹ The quantity μ corresponds to β of Ref. [9]. We have changed the symbol in order to avoid confusion with Eq. (5).

Within this limit, s_N and s_l are combined into a single quantity $B = s_l s_N^\nu$, where $\nu (= 0.588)$ is the excluded volume critical exponent. When considering the ratio, S/S_0 , where S_0 is the radius of gyration at an infinite dilution, B is cancelled and the following is obtained [9]

$$\frac{S^2}{S_0^2} = 1.30w^{-1} \left[\frac{w}{\frac{9}{8} + \frac{1}{4} \frac{w^{1/2}}{(1+w^{1/2})}} \right]^{2\nu} \frac{[1 + \Delta(w)]}{[1 + \Delta(1)]}, \quad (2)$$

where $\Delta(w)$ is a function of polydispersity for monodisperse systems and is given by [9]

$$\Delta(w) = 0.062 - 0.240w^{1/2} - 0.008w + 0.265w^{3/2} - 0.142w^2, \quad (3i)$$

while for exponential chain length distribution²

$$\Delta(w) = 0.062 + 0.173w - 0.141w^2, \quad 0 \leq w \leq 1. \quad (3ii)$$

Instead of w , which is not a measurable quantity, it is useful to express macroscopic properties in terms of the overlap parameter, s . Using the framework of Schäfer's theory, for $f = 1$, s can be written [9]

$$s = 0.5(1-w)w^{1-3\nu} \left[\frac{9}{8} + \frac{1}{4} \frac{w^{1/2}}{(1+w^{1/2})} \right]^{3\nu} \quad (4)$$

and can be expressed in terms of experimental variables as

$$s = \beta^3 c M_n^{3\nu-1}, \quad (5)$$

where c is the polymer concentration in g/ml and M_n is the number-averaged molecular weight. Here, β is a non-universal quantity ($\beta \propto B$) that cannot be determined theoretically and must be obtained by adjusting the experimental data to the theoretical expressions. We note, however, that β will be independent of both molecular weight and concentration. Further, we note that Eqs. (2)–(4) define the radius of gyration as a universal function of s .

We also used these results to interpret the dynamic properties of polymers in solution. As shown in the appendix, we used the De Gennes's reptation theory to obtain the following relationship between the gyration radius and the viscosity (Eq. (6)) and the relaxation time (Eq. (7))

$$\frac{\eta_{sp}}{[\eta]c} = \left(\frac{S^2}{S_0^2} \right)^{\frac{3\nu-4}{2\nu-1}}, \quad (6)$$

$$\frac{\tau}{\tau_0} = \left(\frac{S^2}{S_0^2} \right)^{\frac{3\nu-3}{2\nu-1}}, \quad (7)$$

where η_{sp} and $[\eta]$ are the specific and intrinsic viscosity, respectively, τ is the longest relaxation time, and τ_0 is its

² This expression of $\Delta(w)$ was obtained from Fig. 6 in [9] adjusting a polynomial function.

Table 1
Characteristics of the samples used in this work

Sample	$M_w/$ (10^4 g mol $^{-1}$) ^a	$M_n/$ (10^4 g mol $^{-1}$)	M_w/M_n	$[\eta]/$ (cm 3 g)
I-2	30.7	14.3 ^b	2.14	90 ± 29
I-3	96	57.5 ^c	1.67	1839 ± 22
I-8	42	21.7 ^b	1.94	1111 ± 5
I-9	45	25.0 ^c	1.80	1088 ± 24
I-10	76	44.7 ^c	1.71	1778 ± 30
I-12	45	25.1 ^c	1.80	915 ± 44
I-16	35.3	18.8 ^c	1.88	911 ± 21

^a Determined by intrinsic viscometry of solutions in acetone.

^b Determined by membrane osmometry in isophorone solutions [10–13].

^c Determined by size exclusion chromatography.

value at infinite dilution. These equations hold at the same levels as the scaling theory; their use avoids introduction of additional adjustable quantities; and known limiting behavior of both dilute and semidilute solutions are satisfied (see Eqs. (A13)–(A17)).

Although this approach does not constitute a unified renormalization group description of the excluded volume or the hydrodynamic and entanglement effects, it has advantages over other theoretical treatments: from the point of view of experimentation, the existence of *only one* adjustable parameter, and the inclusion of the polydispersity effects are advantageous. In contrast, this theory treats the double crossover in concentration and temperature in a unified form.

3. Experimental section

3.1. Materials

Samples of cellulose trinitrate polymer containing $13.9 \pm 0.5\%$ nitrogen were prepared from native cotton as previously described [1,17]. The samples were characterized using size-exclusion chromatography and intrinsic viscometry of tetrahydrofuran and acetone solutions. Values of M_w were calculated using the following relations [18]: $[\eta] = 4.46 (\text{DP}_w)^{0.76}$ and $M_w = \text{DP}_w M_0$, where $[\eta]$ is the intrinsic viscosity, $M_0 = 294$ and DP_w is the degree of polymerization. The number-averaged molecular weight (M_n) of two samples was determined from membrane osmometry of isophorone (3,5,5-trimethylcyclohexenone) solutions

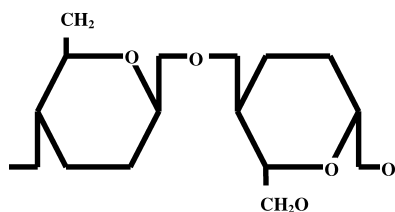


Fig. 1. Schematic diagram of the repeating unit of cellobiose.

prepared by shaking the solvent distillate for 48 h at 30°C. Table 1 shows the characteristics of the samples used.

3.2. Measurements

The intrinsic viscosity $[\eta]$ was determined using Schultz–Blaschke's equation [19]

$$\frac{\eta_{sp}}{c} = [\eta] + [\eta]k_{SB}\eta_{sp}, \quad (8)$$

where c is the solution concentration, η_{sp} is the specific viscosity, and k_{SB} is Schultz–Blaschke's constant. Flow times were measured using an Ostwald viscometer. The flow time of the pure solvent was always higher than 150 s; consequently, kinetic energy corrections could be neglected [19]. The Newtonian viscosity was obtained with a rotoviscometer Haake RV2.

Dielectric measurements were made over a frequency range between 5 Hz and 100 KHz using a Hewlett Packard LF4192A impedance bridge. In order to eliminate the effects of polarization, a cell with a variable gap between electrodes was used. We assumed the following relationship [20]:

$$\frac{1}{C} = \frac{1}{C_p} + \frac{K}{\epsilon}d, \quad (9)$$

where C is the measured capacitance, C_p , the polarized capacitance, K , the cell constant, ϵ , the dielectric permittivity, and d , the distance between the electrodes. We measured capacitance as a function of frequency in the pure solvent and in the solutions using five different distances between electrodes. All measurements were made at 30°C. Because we were interested in the value of the permittivity relative to the solvent, actual values of K could be obtained without calibration.

4. Results

4.1. Analysis of dipole moment

Molecules belonging to Type A according to Stockmayer's classification [21,22] have a dipole component *parallel* to the contour of the backbone chain. Therefore, relaxation behavior of μ (should be identical to that of r_n). The most important consequence of this circumstance is that the relaxation time is dependent upon the molecular weight of the polymer. Molecules having dipole moments perpendicular to the backbone (Types B and C), by contrast, exhibit relaxation times independent of molecular weight.

Cellulose ethers and esters are known to be Type A polymers [23]. Fig. 1 shows the repeat unit of cellobiose, which consists of two glucose rings connected by an oxygen bridge. The axis of the dipole moment should be along the C₁–C₄ line. Lateral groups and cyclic oxygen are opposing (β configuration), and their perpendicular dipole moments are therefore cancelled. The parallel dipole moment is due

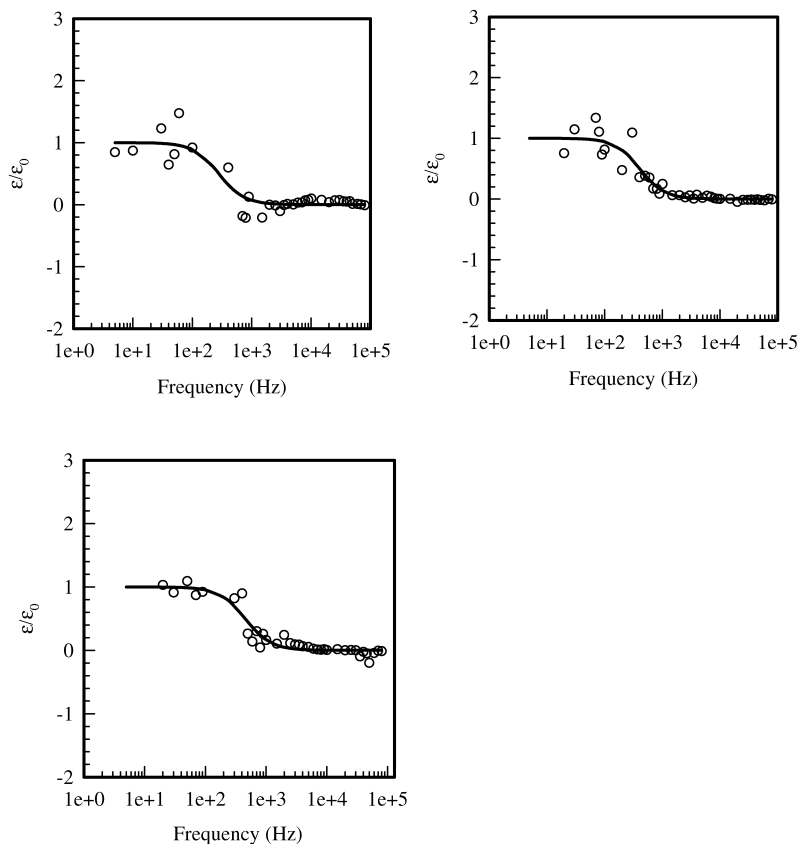


Fig. 2. Representative results depicting dielectric relaxation. Open circles are the experimental points, while the line is the fitted curve of a Debye type relaxation.

to the oxygen atoms joining the glucose rings, and the polymer chain can be considered to be formed by inverse Type A sequences.

We computed the dipole moment of the cellobiose using the AM1 semiempirical method running in PC Spartan-Plus (Wave function Inc., Irvine, CA), and found that it indeed lies in the direction of the line connecting carbon atoms C₁–C₄ of the glycosidic linkage, which confirms that this is a Type A polymer. Nonetheless, Type B and Type C contributions would be expected from the partial substitution of OH groups, and dipolar relaxation of these modes should be found at high frequencies.

We also note that a Type B dipole, ascribable to the overall rotation of the polymer molecule, may be evident at low frequency relaxation times. At infinite dilution, Type A and Type B relaxation modes would both depend on molecular weight, and consequently, we would be unable to distinguish one from the other. In contrast, we expect that as the polymer concentration increases, the Type B relaxation time grows more rapidly, but would be below the lowest frequency limit. In any case, as the absolute value of the Type B dipole is much lower than that of the type A one, the contribution made by the Type B dipole to the relaxation process will be negligible.

4.2. Determination of relaxation times

Relaxation times were calculated by fitting Debye's curve to the experimental data

$$\frac{\varepsilon - \varepsilon_{\infty}}{\varepsilon_0 - \varepsilon_{\infty}} = \frac{1}{1 + \omega^2 \tau^2}, \quad (10)$$

where ε_0 , ε_{∞} , and τ (the static and infinite permittivity and the relaxation time, respectively) were taken as adjustable parameters.

Fig. 2 shows some typical plots of $\varepsilon_r (= \varepsilon_{\text{soln}}/\varepsilon_{\text{solv}})$ expressed as a function of the frequency (ω). Although electrode polarization caused the data to be somewhat scattered at the initial part of the curve, the results appear to be reliable. Relaxation times at infinite dilution were determined by semilogarithmic extrapolation to back zero concentration (Fig. 3).

4.3. Evaluation of β

Fig. 4 shows $\eta_{sp}/(c[\eta])$ expressed as a function of the overlap parameter, $s (= \beta^3 c M_n^{3\nu-1})$. The continuous line indicates the theoretical prediction calculated from Eqs. (2)–(4) and (6). The parameter, β (was fitted to the experimental data for each molecular weight (Table 2). These

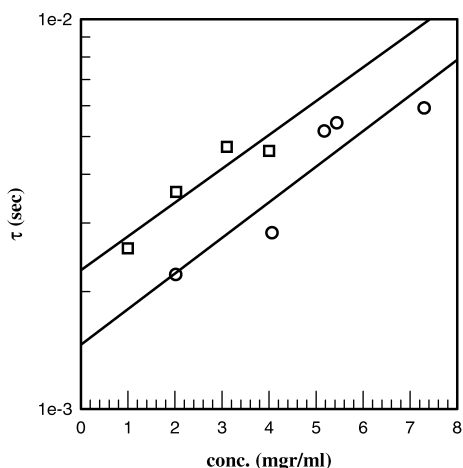


Fig. 3. Semilogarithmic plot showing relaxation time expressed as a function of polymer concentration. The data are extrapolated back to zero concentration.

values were then used to translate the τ/τ_0 data (Fig. 5). The line depicted in Fig. 5 represents the theoretical prediction based on Eqs. (2)–(7).

5. Discussion and conclusions

We applied the renormalization group theory to data describing the viscosity and the relaxation times of polymer solutions in the dilute-to-semidilute crossover; this entailed

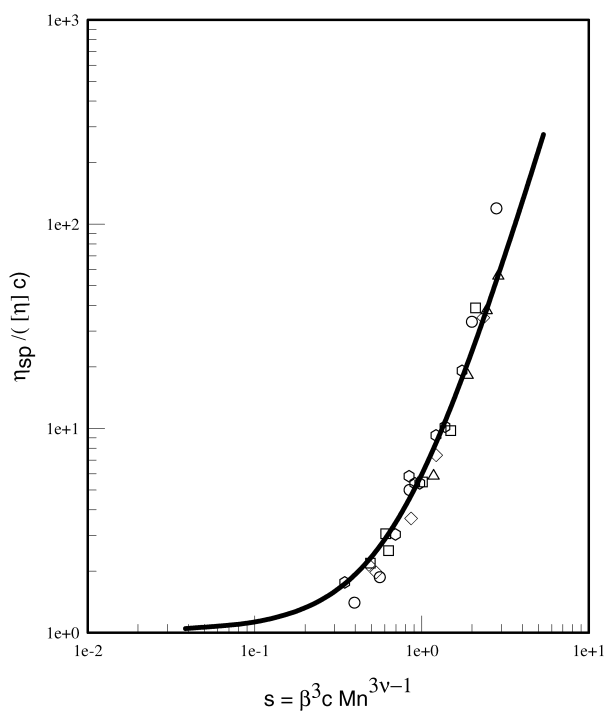


Fig. 4. Normalized viscosity function expressed as an overlap parameter. The value of β corresponds to those indicated in Table 2. The line is the theoretical prediction. \circ Sample I-2; \square Sample I-3; \triangle Sample I-8; ∇ Sample I-10; \diamond Sample I-12.

using De Gennes's blobs model to connect the dynamic and conformational quantities. We found adequate agreement between the experimental results and theoretical predictions showing universal behavior. The values of β were independent of molecular weight and polymer concentration, and they could be used to describe a variety of dynamic properties, suggesting that only one scaling variable is necessary for such purpose.

Throughout this work, we used the naive reptation model. Currently, the existence of fluctuations in chain contour effects is accepted [24,25] for melted polymers. In order to take these effects into account, it was necessary to consider the existence of two relaxation times, each of which was dependent on the entanglement density even in semidilute solutions. This introduces a slight ambiguity into our analysis; fortunately however, the degree of overlap was small and essentially involved only dilute solution, for which the renormalization theory applies.

Finally, we note that our analysis revealed that the elastic modulus could also be studied using the scheme presented here (see the appendix). Thus, we should be able to obtain measurements of viscosity, relaxation times and elastic modulus using the same system.

Acknowledgements

This work was partly supported by the Consejo Nacional de Investigaciones Científicas y Técnicas of Argentina (CONICET). RVF and JRG are members of the Carrera del Investigador of CONCIET and IMI is fellow of the same institution.

Appendix A

According to the reptation model, as a macromolecular chain diffuses, it is continuously vacating a tube-like region within the solvent and occupying a new one. The dynamics of this process was discussed by de Gennes to determine the low-frequency properties of entangled polymer using two concentration-dependent parameters, a and N_e (the distance and the number of monomers between entanglements, respectively). Using this method, we derived the known results for the viscosity of solutions in good solvents. Consider a chain consisting of a series of segments having a size proportional to a . The total number of segments is proportional to N/N_e , and if the hydrodynamic interactions in the interior of the segments are unscreened, the chain friction coefficient f_{chain} will vary according to Stokes and Einstein

$$f_{\text{chain}} \propto 6 \pi \eta_s a \left(\frac{N}{N_e} \right) \propto \frac{kT}{D_{\text{tube}}}, \quad (\text{A1})$$

where N is the number of monomers in the chain and η_s is the solvent viscosity. To disengage from a given tube, the molecule must diffuse a distance on the order of the chain

Table 2
Values of β corresponding to each sample computed from viscosity measurements

Sample	β
I-2	0.27
I-3	0.27
I-8	0.27
I-10	0.29
I-12	0.27

length aN/N_e . Therefore, according to Einstein, the longest relaxation time τ_r is now

$$\tau_r \propto \frac{1}{2} \frac{\left(\frac{a}{N_e} N\right)^2}{D_{\text{tube}}} \quad (\text{A2})$$

The polymer contribution to the solution viscosity, $\eta - \eta_s$, is given by Maxwell's relation

$$\eta - \eta_s \propto \tau_r G, \quad (\text{A3})$$

where G is the relaxation strength associated with τ_r , and η is the solution viscosity. The modulus G is proportional to the number-concentration of entanglement

$$G \propto \frac{c}{N_e}, \quad (\text{A4})$$

where c is the weight-polymer concentration. From Eqs. (A1)–(A4) it is possible to obtain the reduced viscosity as

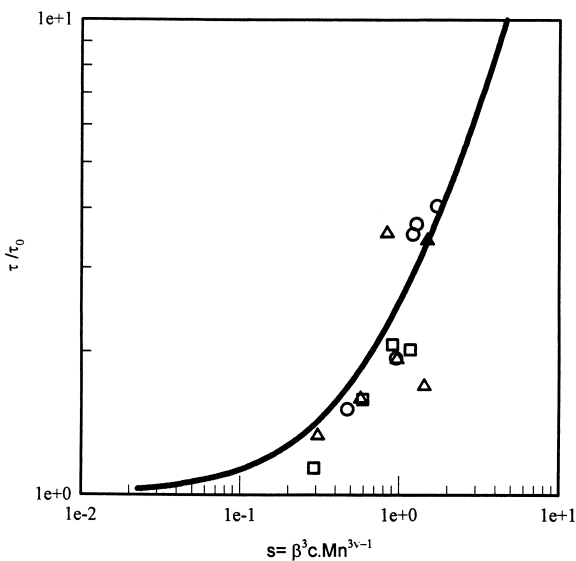


Fig. 5. Reduction of relaxation time as a function of the overlap parameter using the values of β also used in Fig. 4. \circ Sample I-16; \square Sample I-9; Δ Sample I-12.

follows:

$$\frac{\eta_{\text{sp}}}{c} \propto \frac{\left(\frac{Na}{N_e}\right)^3}{N_e} \quad (\text{A5})$$

To define the viscosity in terms of molecular parameters, it is argued that the distance a is proportional to the correlation length. In other words, the aforementioned chain segments correspond to blobs in the static description of semidilute solutions. Accordingly, the above-introduced parameters, N , N_e and a are interrelated in the following way:

$$a \propto N_e^\nu; \quad S_0 \propto N^\nu; \quad S \propto a \left(\frac{N}{N_e}\right)^{1/2}, \quad (\text{A6})$$

where S is the radius of gyration of the chain, S_0 its value in very dilute solution and ν ($=0.588$) the excluded volume exponent. By combining Eqs. (A5) and (A6) we obtain

$$\frac{\eta_{\text{sp}}}{c} = \frac{S_0^3}{N} \left(\frac{S^2}{S_0^2}\right)^{\frac{3\nu-4}{2\nu-1}} \quad (\text{A7})$$

For very dilute solution, Zimm's formulation for the intrinsic viscosity is obtained

$$[\eta] \propto \frac{S_0^3}{N} \quad (\text{A8})$$

Eqs. (A7) and (A8) lead to

$$\frac{\eta_{\text{sp}}}{c[\eta]} = \left(\frac{S^2}{S_0^2}\right)^{\frac{3\nu-4}{2\nu-1}} \quad (\text{A9})$$

Further, with Eqs. (A1), (A2) and (A6) we can obtain

$$\tau_r \propto a^3 \left(\frac{N}{N_e}\right)^3 \frac{\eta_s}{kT} \propto \left(\frac{S^2}{S_0^2}\right)^{\frac{3\nu-4}{2\nu-1}} S_0^3 \frac{\eta_s}{kT} \quad (\text{A10})$$

Also for very dilute solutions ($c \rightarrow 0$) we have

$$\tau_0 \propto \frac{\eta_s}{kT} S_0^3 \quad (\text{A11})$$

Finally, Eqs. (A10) and (A11) lead to

$$\frac{\tau}{\tau_0} = \left(\frac{S^2}{S_0^2}\right)^{\frac{3\nu-4}{2\nu-1}} \quad (\text{A12})$$

We could analyze limiting behavior. For dilute solutions ($w \rightarrow 1$; $s \rightarrow 0$); therefore, Eqs. (6) and (A11) can be written

$$\eta_{\text{sp}}/(c[\eta]) = 1 + 2(4 - 3\nu)s/(1, 25)3\nu, \quad (\text{A13})$$

which is Huggins's equation [21]:

$$\frac{\eta_{\text{sp}}}{c[\eta]} = [\eta] + K_H[\eta]^2 c, \quad (\text{A14})$$

where K_H is Huggin's constant. Combining Eqs. (A13) and

(A14) with the definition of s we obtain

$$K_H = \frac{2(4 - 3\nu)}{1.25^{3\nu}} \beta^3 \frac{M_n^{3\nu-1}}{[\eta]} \quad (\text{A15})$$

In the semidilute limit ($w \rightarrow 0$; $s \rightarrow 0$), Eqs. (2), (3) and (5) are reduced to

$$\eta_{sp}(c[\eta]) \propto w^{(3\nu-4)} \propto s^{((3\nu-4)/(1-3\nu))} \quad (\text{A16})$$

and De Gennes' limiting relation is obtained:

$$\eta_{sp} \rightarrow M^3 c^{3/(3\nu-1)} (s \rightarrow 0) \quad (\text{A17})$$

References

- [1] Yamakawa H. Modern theory of polymer solutions. New York: Harper and Row, 1971.
- [2] Doi M, Edwards SF. The theory of polymer dynamics. Oxford: Oxford University Press, 1986.
- [3] Gennes PG. Scaling concepts in polymer physics. Ithaca, NY: Cornell University Press, 1979.
- [4] des Cloizeaux J. J Phys (France) 1975;36:281.
- [5] Shiwa Y. Phys Rev Lett 1986;58:2102.
- [6] Shiwa Y, Oono Y, Baldwin PR. Macromolecules 1988;21:208.
- [7] Nyström B. Macromolecules 1993;26:3784.
- [8] Schäfer L. Macromolecules 1982;15:652.
- [9] Schäfer L. Macromolecules 1984;17:1357.
- [10] Kappeler C, Schäfer L. Macromolecules 1990;23:2766.
- [11] Schäfer L, Kappeler C. Colloid Polym Sci 1990;268:995–1017.
- [12] Schäfer L, Lehr U, Kappeler C. J Phys (France) I 1991;1:211.
- [13] Schäfer L, Kappeler C. J Chem Phys 1993;99:8.
- [14] Grigera TS, Irurzun IM, Cortizo MS, Figini RV, Marx-Figini M, to be published.
- [15] Noda I, Kato N, Kitano T, Nagasawa M. Macromolecules 1981;14:668.
- [16] Takahashi Y, Isono Y, Noda I, Nagasawa T. Macromolecules 1985;18:1002.
- [17] Marx M, Schulz GV. Die Makromol Chemie 1959;31:140.
- [18] Marx-Figini M, Schulz GV. Die Makromol Chemie 1962;54:102.
- [19] Slade Jr. PE, editor. Polymer molecular weight, Part II. New York: Marcel Dekker, 1975.
- [20] Shaw TM. J Chem Phys 1942;10:609.
- [21] Stockmayer WH. Pure Appl Chem 1962;15:539.
- [22] Stockmayer WH, Baur ME. J Am Chem Soc 1964;86:3485.
- [23] Scherer PC, Levi DW, Hawkins MC. J Polym Sci 1957;24:19.
- [24] Doi M. J Polym Sci, Polym Lett 1981;19:265.
- [25] Wool RP. Macromolecules 1993;26:1564.